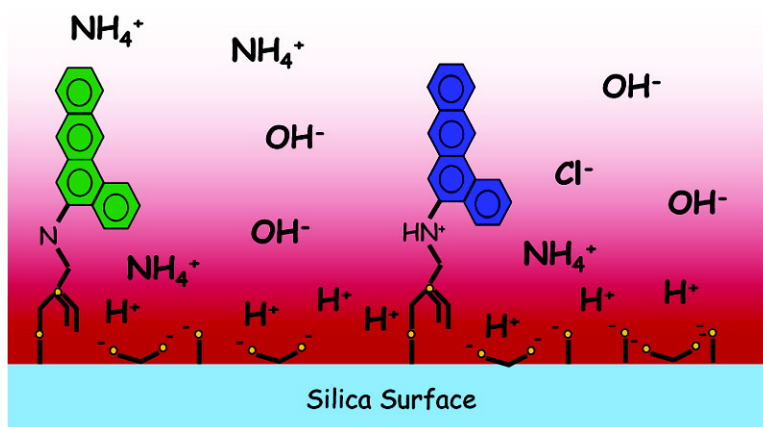


Interfacial pH at an Isolated Silica–Water Surface

Josephine P. O'Reilly, Craig P. Butts, Ian A. I'Anso, and Andrew M. Shaw

J. Am. Chem. Soc., **2005**, 127 (6), 1632-1633 • DOI: 10.1021/ja0443326 • Publication Date (Web): 22 January 2005

Downloaded from <http://pubs.acs.org> on March 24, 2009



More About This Article

Additional resources and features associated with this article are available within the HTML version:

- Supporting Information
- Links to the 8 articles that cite this article, as of the time of this article download
- Access to high resolution figures
- Links to articles and content related to this article
- Copyright permission to reproduce figures and/or text from this article

[View the Full Text HTML](#)

Interfacial pH at an Isolated Silica–Water Surface

Josephine P. O'Reilly, Craig P. Butts, Ian A. l'Anson, and Andrew M. Shaw*

School of Biological and Chemical Sciences, University of Exeter, Stocker Road, Exeter, EX4 4QD, UK

Received September 17, 2004; E-mail: andrew.m.shaw@exeter.ac.uk

An isolated silica–water interface becomes electrically charged in solution due to the presence of deprotonated silanol groups on the surface.¹ The surface charge depends on the pK_a of the silanol groups, the pH at the interface, and the silanol group surface density, all of which have been measured by complementary optical techniques both direct^{2,3} and indirect.⁴ When the surface is deprotonated, the negative charge creates a potential difference between the surface and the bulk. Positive counterions are attracted by the surface potential to the interface and form a diffuse or layered structure described by the Gouy–Chapman–Stern theory.⁵ Protons are attracted to the interface as counterions, and the resulting interfacial pH should be consequently lower than that of the bulk pH. The silanol group can also act as a binding site to functionalize the surface and control the surface properties.^{6–9} We have tethered a derivative of the pH-sensitive dye Nile Blue to the silica surface and monitored its absorbance at a fixed wavelength, 637 nm. This provides an optical method that is sensitive to the interfacial pH directly. The absolute absorbance at the interface was measured using evanescent wave cavity ring-down spectroscopy² (e-CRDS). The bulk pH was varied from 1 to 10, allowing the silica surface to be titrated. The observed absorbance at high pH indicates an interfacial pH that is two pH units lower than the bulk value for the fully charged surface, consistent with a surface potential of order $-120 \text{ mV}^{2,3}$ relative to zero in the bulk. A stable charged near-surface layer is formed that is not disrupted on reversing the titration.

The silica surface comprises two types of Si–OH groups designated Q3 for $(\text{SiO})_3\text{–SiOH}$ structure and Q2 for $(\text{SiO})_2\text{–Si(OH)}_2$ structure.⁹ Second harmonic generation measurements³ suggest a typical site density is on the order of 4 nm^{-2} with a Q2:Q3 ratio of 3:1. Each group has a different pK_a : Q3 has a pK_a of 4.5 and Q2 has a pK_a of 8.5.³ A derivative (**1**) of the pH-sensitive dye Nile Blue, Figure 1, was prepared for tethering to the silica surface.

The triethoxysilane group was chosen in preference to chlorosilane derivatives to minimize the degree of self-polymerization of the silane species on the surface.¹¹

The preparation of **1** was adapted from that reported by Nakazumi et al.¹² and involved reaction of Meldola's blue (0.2 g, 0.64 mmol) and (3-aminopropyl)triethoxysilane (0.13 g, 0.64 mmol) at reflux in methanol solution (10 cm^3) under air for 30 min. The resultant solution was washed with hexane and ethyl acetate until the washings became colorless. The solvent was removed in vacuo and the resultant solid dried under vacuum. A ^1H NMR spectrum was obtained and the derivative characterized fully according to standard organic synthesis practice. A UV/vis spectrum of **1** showed peak maxima at 592 and 470 nm ($\epsilon = 44770$ and $50750 \text{ M}^{-1} \text{ cm}^{-1}$ respectively). The synthesis yields typically 20%, although higher yields could be obtained using a large excess of (3-aminopropyl)triethoxysilane and isolated by precipitation following the addition of excess THF. Direct measurement of the pK_a of the iminium proton of **1** is not possible due to the partial hydrolysis of the

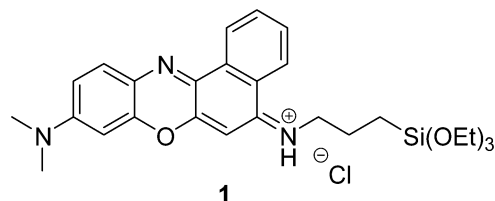


Figure 1. Structure of the Nile Blue derivative **1**.

triethoxysilyl group in basic conditions. However, as the primary iminium ion, Nile Blue, has a pK_a of ~ 11 ,¹¹ the effect of the alkyl group is such that the pK_a of the secondary iminium group of salt **1** can reasonably be estimated at around 9.

The molecule **1** was tethered onto the surface of a Schott glass Dove prism¹ before transfer to the e-CRDS Dove cavity. The principles of e-CRDS have been detailed elsewhere² and will only be described briefly here. Two high-reflectivity mirrors (99.95%) are placed opposite one another to form a linear optical cavity into which light from a broad-band cw diode laser ($637 \pm 2 \text{ nm}$) is introduced. The bandwidth of the laser is sufficiently large to overlap $\sim 10^3$ cavity modes in a free-running configuration and light always enters the cavity, building up to an intensity determined by the cavity Q-factor. The laser is switched off and on at a repetition rate of 6 kHz, and the radiation intensity in the cavity decays with a ring-down time, τ , determined similarly by the Q-factor. A Dove prism is introduced into the cavity as a total internal reflection element that generates an evanescent wave at the interface between the glass and the water. The evanescent wave penetrates 186 nm into the interface above the prism determined by the ratio of the refractive indices of the two media and the angle of incidence of the refracting radiation. Molecules that absorb at the laser wavelength and are present within the evanescent field remove radiation from the cavity decreasing the ring-down time, τ . The change in τ is directly related to the absorbance of the species and the concentration profile of the species at the interface.

A series of conditions was investigated for the tethering procedure including incubation time, bulk pH, temperature, and concentration of the Nile Blue derivative **1**. The extinction coefficient for the Nile Blue derivative **1** is assumed to be similar to that of Nile Blue at 637 nm, $\epsilon = 27029 \text{ M}^{-1} \text{ cm}^{-1}$, from which the concentration in the solution during incubation can be derived. The surface tethering was performed at pH 10 and $65 \text{ }^\circ\text{C}$ from a bulk solution concentration of 90 nM. The incubation kinetics can be fitted to a first-order rate law consistent with a tethering rate constant $k_t = (1.84 \pm 0.33) \times 10^{18} \text{ molecules cm}^{-2} \text{ s}^{-1}$. This rate constant has not been corrected for the Boltzmann-enhanced surface concentration.

The maximum absorbance observed from deposition of the derivative is 1.6×10^{-3} , at the deposition pH, and, assuming a 1 nm^{-2} silanol site density, this indicates a surface coverage of 5×10^{-5} of a monolayer. Deposition from the 90 nM solution and the resultant low surface coverage, suggests the derivative **1** will not

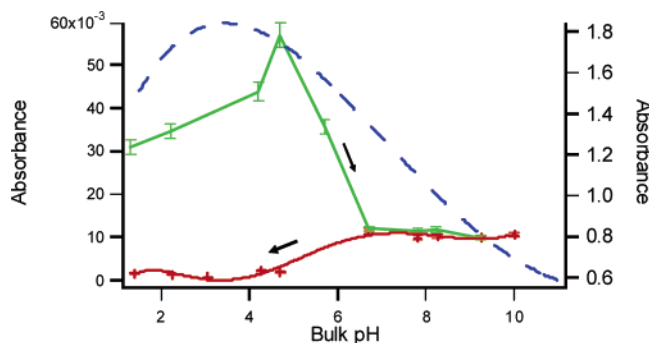


Figure 2. Titration of the silica–water interface. (a) Upper trace: increasing pH (green curve), (b) lower trace: decreasing pH (red curve), (c) dashed trace: solution pH - absorbance variation corrected for surface pH (dashed blue lines).

cluster on binding. Hence, the surface charging properties are still determined by the intrinsic SiOH properties, and the tethered chromophore does not perturb the interface significantly.

The variation of absorbance of the tethered species as a function of bulk pH is shown in Figure 2. The e-CRDS sensitivity and the absorbance change from pH 5 to 6.5 in trace (a) suggests that a pH change on the order of 0.001 pH units can be detected. The bulk pH was adjusted with HCl and NH_4OH starting at low pH, flowing fresh solutions of different pH at each point. The variation of the interface absorbance with increasing pH is seen in trace (a) and shows an initial increase to pH 5 followed by a decrease in absorbance from pH 5 to 6.5. However, when the pH is reduced from pH 10 \rightarrow 1, trace (b), the absorbance does not recover and shows a distinct hysteresis attributed to the charging properties of the layer structure. The surface can be cleaned with methanol and the titration repeated, proving the derivative has not been hydrolyzed.

Titration of the surface silanol groups from low to high pH varies the charge of the surface and hence the surface potential. The variation in surface potential with bulk pH has been determined previously^{2,3} and can be used to determine the enhanced concentrations of positively charged species at the surface and hence the interfacial pH. The absorbance of the derivative **1** in the bulk has been corrected for the interfacial pH using the Boltzmann equation at each surface potential⁵ and can be seen in trace (c), Figure 2. It is assumed that the variation of the tethered derivative absorbance at the interface is the same as that of the bulk, given the low surface coverage. The measured absorbance maximum in trace (a) compares well with the absorbance maximum of the corrected solution-phase absorbance in trace (c), showing directly the effect of the surface charge on the interfacial pH.

During the decreasing pH titration, trace (b), the absorbance decreases at lower bulk pH, suggesting an increase in the interfacial pH. This increase in interfacial pH is consistent with a stable charged layer at the surface with a smaller volume. The diffuse

layer description⁵ of the interface uses the Debye length to estimate the thickness of the diffuse layer, and for the concentrations of solutes used in the titration, the Debye length varies from 1.7 nm at pH 1.5 to over 900 nm for pure water, pH 7, to 30 nm for pH 10. However, the tethered chromophore is only sensitive to pH in the local environment within 1 nm of the surface and away from the variations in the bilayer thickness in a region clearly dominated by a stable near-surface bilayer. A similar oriented water layer was observed previously by SHG measurements.³

AFM images of the clean prism surface indicated a roughness parameter of 3.35 ± 0.93 nm, suggesting extensive surface features providing local environments for the chromophore with local charge density and surface potential, although these will be averaged over the area of the evanescent field, 0.75 mm^2 . The local environment around the tethered chromophore will have a high positive counterion concentration of order 11 M for a fully dissociated surface. This large counterion concentration may cause a solvatochromic shift in the absorption spectrum and hence absorbance at 637 nm. The optical measurement of the interfacial pH is directly sensitive both to the change in the structure of the charged interface and to the change in the spectrum of the chromophore. A detailed analysis of the shape of both traces (a) and (b) will include this effect, but it would appear to be small. A large solvatochromic shift would have a pronounced effect over the entire pH range of the titration. Trace (a) is dominated by the deprotonation of the dye with a single $\text{p}K_a$ in equilibrium with the interfacial pH, while trace (b) shows no pronounced shift. Future measurement of the absorption spectrum of the tethered molecule will prove to be a very sensitive probe of the interface environment of the chromophore and interfacial pH.

Acknowledgment. We thank the ESPRC for funding this research.

References

- (1) Iller, R. K. *The Chemistry of Silica*; Wiley & Sons: New York, 1979; pp 623–729.
- (2) Shaw, A. M.; Hannon, T. E.; Li, F.; Zare, R. N. *J. Phys. Chem. B* **2003**, *107*, 7070–7075.
- (3) Ong, S.; Zhao, X.; Eiseenthal, K. B. *Chem. Phys. Lett.* **1992**, *191*, 327–335.
- (4) Cremer, P. S.; Boxer, S. G. *J. Phys. Chem. B* **1999**, *103*, 2554–2559.
- (5) Bard, A. J.; Faulkner, L. R. *Electrochemical Methods: Fundamentals and Applications*, 2nd ed.; Wiley & Sons: New York 2001; Chapter 12.
- (6) Flink, S.; van Veggel, F. C. J. M.; Reinhoudt, D. N. *J. Phys. Org. Chem.* **2001**, *14*, 407–415.
- (7) Silberzan, P.; Léger, L.; Ausserré, D.; Benattar, J. J. *Langmuir* **1991**, *7*, 1647–1651.
- (8) Bryant, M. A.; Crooks, R. M. *Langmuir* **1993**, *9*, 385–387.
- (9) Sharma, A.; Jain, H.; Miller, A. C. *Surf. Interface Anal.* **2001**, *31*, 369–374.
- (10) Macial, G. E. In *Encyclopedia of NMR*; Grant, D. M., Harris, R. K., Eds.; Wiley: Chichester, 1996.
- (11) Tripp, C. P.; Kazamair, P.; Hair, M. L. *Langmuir* **1996**, *12*, 6407–6409.
- (12) Nakazumi, H.; Amano, S. *Chem. Commun.* **1992**, *15*, 1079–1080.
- (13) Mendham, J.; Denney, R. C.; Barnes, J. D.; Thomas, M. *Vogel's Textbook of Quantitative Chemical Analysis*, 6th ed.; Prentice Hall: New York, 2000.

JA0443326